



# Fabrication and Characterization of Poly (Lactic acid)/Propylparaben Composite for Active Food Packaging Application

Usman Lawal<sup>1,2,3</sup> · Vijay Robert<sup>1</sup> · Akshai Gopi<sup>1,2</sup> · Sravanthi Loganathan<sup>1,2</sup> · Ravi Babu Valapa<sup>1,2</sup>

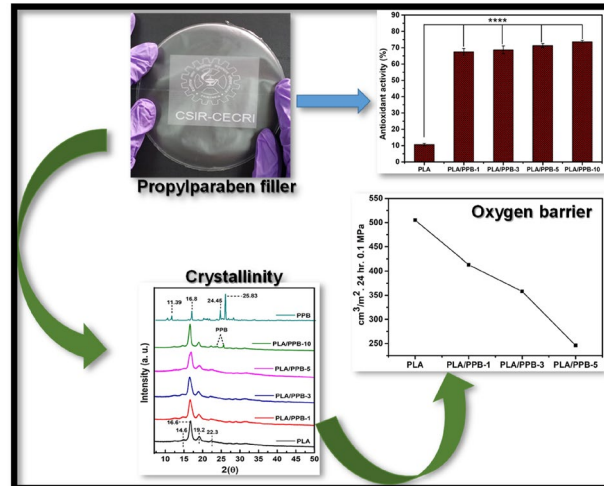
Accepted: 28 November 2023 / Published online: 21 January 2024

© The Author(s), under exclusive licence to Springer Science+Business Media, LLC, part of Springer Nature 2024

## Abstract

Sustainable poly(lactic acid) (PLA)/propylparaben (PPB) composite based films were fabricated via solution casting approach. The assessment of PLA/PPB composite films in terms of active food packaging characteristics like thermal, mechanical, UV–Vis, oxygen barrier, anti-bacterial as well as anti-oxidant effect is carried out. The PLA/PPB-5 composite film resulted in three-fold (23%) increase of elongation-at-break while maintaining a tensile strength (42 MPa) in comparison with PLA film. Consequently, the PLA/PPB-5 composite film displayed a 70% UV–B blockage and reduced the oxygen transmission rate by 52% as compared to PLA film. Further, the PLA/PPB-5 composite film exhibited significant improvement (52%) in the radical scavenging activity which can be really helpful to keep the food products fresh for longer periods. The PLA/PPB filler showed good antibacterial activity against food-borne bacteria [*Staphylococcus aureus* and *Escherichia coli*]. The fabricated PLA/PPB composite films have shown desirable active food packaging characteristics and therefore may be suitable for food packaging applications.

## Graphical Abstract



**Keywords** Poly (Lactic acid) · Propylparaben · Biocomposite · UV–shielding · Antibacterial and packaging

## Introduction

Conventional plastics have demonstrated high versatility since their commercial introduction, as they are light in weight and present suitable mechanical as well as barrier

Extended author information available on the last page of the article

properties. Plastics have found a wide variety of use in food and logistics packaging, medical equipment, construction, and agriculture [1, 2]. Conventional plastics derived from petrochemical resources are mostly non-biodegradable and thus raise a serious environmental concern. This further led to increased interest for biodegradable polymers based on renewable sources for packaging applications [3, 4]. Poly (lactic acid) (PLA) has emerged as a promising biopolymer to replace petroleum-based polymers due to its compostability, low carbon footprint, mechanical properties, easy processability and inexpensive nature in comparison with other polymers [5]. However, PLA still exhibits some drawbacks such as high brittleness, poor elongation at break and oxygen barrier properties, which will hinder its wide applicability for food packaging applications [6, 7].

To address these issues, PLA has been combined with other polymers [8], both organic and inorganic fillers [9], plant and animal extracts [10], and incorporating with bio-fillers [11] to improve active packaging film properties such as UV-light blocking, antioxidant, and antimicrobial activity. Blown film extrusion process was used to prepare poly (lactic acid)/poly (butylene-succinate-co-adipate) (PLA/PBSA) blends containing 3 wt% and 6 wt% of thymol. The PLA/PBSA/thymol blends were shown to exhibit in vitro antifungal activity against *Aspergillus* spp. and *Penicillium* spp. The antifungal activity of thymol is due to the hydroxyl groups of volatile compound and presence of a delocalized system allowing the hydroxyl group to release its proton. The composite films were found to present effective gas barrier properties by reducing the water vapor (33%), oxygen (24.5%) and carbon dioxide (36.4%) permeation in comparison with PLA. Studies on the effect of this composite as packaging material for bread showed significant improvement in active packaging property in comparison with PLA [8]. In 2022, Santos et al., studied the antibacterial capabilities of MXene ( $Ti_3C_2T_x$ ) to produce active contact surfaces for food packaging based on PLA polymer. In this work, PLA/MXene films were developed by solution casting process and investigation on its antibacterial activity against *Listeria mono-cytogenes* and *Salmonella enterica* (Gram-positive and Gram-negative, respectively) was carried out. For 0.5 wt% of MXene loading in PLA, 99.99% bactericidal activity was shown against both *Listeria* and *Salmonella* by the composite. Further, the non-cytotoxic nature of the PLA/MXene (0.5 wt%) composite was also confirmed, which recommends its suitability for food packaging application [9].

A three-component filler composed of fumed silica (FS), iron (Fe), and tea polyphenols (TP) was integrated into PLA for preparing active packaging-based composites. Using this, release based active coating formulation was prepared and shown to exhibit ~4-log reduction (99.99%) against Gram-positive (*S. aureus*) and the Gram-negative (*Pseudomonas aeruginosa* and *S. enterica*) bacteria with just

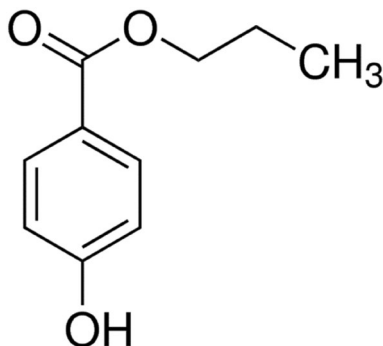
10 wt% loadings of filler in the PLA matrix. This can be related to the generation of noxious reactive oxygen species (ROS) like hydroxyl radical (OH) by the Fe (II) ions exerting antibacterial effects through the causing damage and eventually inhibition. The PLA/FS/Fe/TP composite film also exhibited ~67% increase in antioxidant activity. Green tea polyphenols have the capacity of radical stabilization, which improves free radical scavenging activity [10]. In 2014, Hassan et al., synthesized bio-calcium carbonate (bio- $CaCO_3$ ) through mechanochemical and ultrasonic irradiation techniques from waste eggshells. The bio-calcium carbonates (1–3 wt%) were integrated into Bioplast GS 2189 (PLA/Starch) polymer matrix via solution mixing to improve its mechanical and thermal properties. The Bioplast GS 2189/bio- $CaCO_3$  (2 wt%) exhibited improvement in terms of mechanical characteristics. The flexural strength and modulus were found to be enhanced by 35.3 and 30.5%, respectively. The Bioplast GS 2189/bio- $CaCO_3$  composites films also demonstrated 62% blockage in UV transmission, which signified its potential for active food packaging [11]. PLA/clove essential oil/alkali-treated halloysite nanotube composite films exhibited significant improvement in active packaging properties. The surface hydrophobicity was found to be improved by 20.2%, which in turn reflected enhancement in water vapor barrier by 42.1%. Tremendous improvement in terms of flexibility (682%) was achieved as compared to neat PLA [12].

Recently, food additives are explored as reinforcements in PLA matrix and investigation on their active food packaging characteristics have received considerable attention [13–15]. Bio-based packaging material with capabilities of sensing ammonia vapor and food spoilage have been developed by integrating curcumin into a blend of PLA/polypropylene carbonate (PCC). The presence of curcumin in the PLA matrix was reported to effectively block UV light (98%) which can be attributed to the absorption of UV light by phenolic groups in curcumin. The composites reported excellent transparency as well. The hydrophobic PLA/PCC/Curcumin composites films were shown to exhibit reduction in oxygen permeability values (66% for 40 wt% of PCC). PCC is generally known to exhibit lower oxygen permeability compared to PLA. Hence, when they are blended, the composites exhibit lower oxygen permeability. Further, the PLA/PCC/Curcumin composite films showed better antioxidant property ( $49.3 \pm 2.7\%$  within 24 h) and displayed colour change in response to ammonia vapor released during food spoilage. Owing to the excellent UV blockage,  $O_2$  barrier, antioxidant, and ammonia sensitivity features, it was concluded that PLA/PCC/curcumin composites could effectively be used for active food packaging applications [15].

Parabens belong to the family of esters of para-hydroxybenzoic acid, which include methylparaben, ethyl paraben, propylparaben, butylparaben. Parabens were reported to

exhibit effective antifungal, antimicrobial and preservative features. Among the paraben family, propylparaben (PPB) is a naturally occurring compound found in some plants and insects [16]. Propylparaben have been commonly used as preservatives for several decades in wide range of products like food stuffs, cosmetics, pharmaceuticals, and industrial products [17, 18]. The effect of slow release of PPB from styrene-acrylate polymer coating was used to understand its effect on the inhibition of growth of *Saccharomyces cerevisiae* [19]. All these features speculate that PPB could be explored as additive in the PLA matrix and envisage the active food packaging properties of PLA/PPB composite films, which has not been documented earlier.

In the current work, PLA/PPB composites with different wt% loadings (1, 3, 5, and 10 wt%) of PPB were fabricated using solution casting approach. The influence of wt% loadings of PPB on the physicochemical characteristics of PLA is investigated. Further, thermal, mechanical and oxygen barrier properties of PLA/PPB composite films were also studied. To explore the active food packaging properties of PLA/PPB composite films, examination of UV–Visible light barrier properties, anti-oxidant potential, antibacterial effect along with migration as well as release studies was performed.



Chemical Structure of PPB

## Materials and Methods

### Materials

The bio-polymer matrix poly (lactic acid) (Ingeo™ Biopolymer 4043D) was supplied by NatureWorks LLC, USA [specific gravity of 1.24 g/cc and molecular weight: 160 g/mol]. Propyl-4-hydroxybenzoate or propyl paraben (PPB) was used as an additive in the PLA matrix and supplied by Sigma Aldrich. The organic solvent “chloroform” is used for solubilization of PPB and PLA. For FTIR spectroscopy measurements, potassium bromide (KBr) powder was used. Both the chemicals were procured from Sisco Research Laboratories,

India. The antioxidant activity reagent “2, 2-diphenyl- 1-picrylhydrazyl (DPPH)” was supplied by Sigma Aldrich, USA. For migration analysis, Tenax was used as the dry food simulant and supplied by Sigma Aldrich, USA.

### Preparation of PLA/Propylparaben Composite Films

The solution casting method was used to fabricate the PLA and PLA/PPB composite films. Under ambient circumstances, 1 g of PLA was dissolved in chloroform and homogenized until a clear solution was formed. The resulting solution was then casted onto a flat petri dish and dried at room temperature for 24 h. Following solvent evaporation, the films were peeled off and dried at 40 °C under vacuum for 24 h to allow for complete evaporation of solvent. To fabricate PLA/PPB composite films, different concentrations of PPB (1, 3, 5, and 10 wt% w.r.t. to PLA) were mixed with 30 mL of chloroform and subjected to sonication. For 1 h, the homogenization procedure was continued until a clear solution was achieved. PLA was similarly solubilized with chloroform, as stated herein. Following by this, the two solutions were combined and sonicated for 2 h to achieve appropriate homogenization. The rest of the technique for preparing PLA/PPB composite films is the same as PLA. The as prepared PLA/PPB composite films were named as PLA/PPB-1, PLA/PPB-3, PLA/PPB-5, and PLA/PPB-10, respectively.

### Characterization

#### Thermogravimetric Analysis (TGA)

TG analyzer (NETZCH, Germany & Model: STA 2500) was used to acquire the thermal decomposition profile for PLA and PLA/PPB composite films. The PLA and PLA/PPB composite films ( $5 \pm 0.2$  mg) were weighed, and thermal analysis was carried out in the temperature range of 25 to 600 °C at a heating rate of 10 °C/min. The experiment was carried out in a nitrogen (N<sub>2</sub>) atmosphere with a gas flow rate of 100 mL/min.

#### Differential Scanning Calorimetry (DSC) Analysis

DSC analyser (METTLER TOLEDO, Switzerland & Model: DSC 1) was used to measure the glass transition temperature ( $T_g$ ), cold crystallization temperature ( $T_{cc}$ ), and melting temperature ( $T_m$ ) of PLA and PLA/PPB composite films. Approximately, PLA and PLA/PPB composite films ( $5 \pm 0.2$  mg) were weighed and hermetically sealed in aluminium

pans for this study. The samples were then heated from 25 to 200 °C at a rate of 5 °C/min under N<sub>2</sub> atmosphere (flow rate of 100 mL/min) and kept isothermally at 200 °C for 5 min to erase the thermal history. The second heating cycle

was used to determine the thermal characteristics of PLA and PLA/PPB composite films. The degree of crystallization ( $X_c$ ) for PLA and PLA-PPB composites was thus calculated from Eq. (1):

$$X_c(\%) = \left[ \frac{(\Delta H_m - \Delta H_c)}{\Delta H_{m0}} \right] \times 100 \quad (1)$$

where  $\Delta H_c$  is the enthalpy of crystallization and  $\Delta H_m$  is the enthalpy of fusion, and  $\Delta H_{m0}$  is the theoretical enthalpy of 100% crystalline PLA (93 J/g) [15].

### X-ray Diffraction (XRD) Analysis

XRD analyzer (Bruker, Germany & Model: D8 Advance) was used to obtain the diffraction pattern for PLA and PLA/PPB composite films. The XRD data was acquired in the  $2\theta$  range of  $5\text{--}50^\circ$  with slow scan rate of  $10^\circ \text{ s}^{-1}$ . Under ambient conditions, the instrument was operated at 40 kV and 30 mA.

### Fourier Transform Infrared (FTIR) Spectroscopy

FTIR spectrometer (Bruker, Germany & Model: TENSOR 27) was used to obtain infrared spectra for PLA and PLA/PPB composite films. The measurements were carried out using attenuated total reflectance (ATR) mode. The IR measurements for PLA and PLA/PPB composites samples were performed in the wavenumber region of  $4000\text{--}400 \text{ cm}^{-1}$  with a resolution of  $4 \text{ cm}^{-1}$ . Using KBr powder in pellet mode, the IR spectrum for filler was obtained.

### Morphological Analysis

Field emission Scanning electron microscopy (FE-SEM) (Carl Zeiss, Germany and Model: 27 PerkinElmer Spectrum Two) was utilized to analyse surface and cross-section morphology for PLA and PLA/PPB composite films, with an accelerating voltage of 5 kV. SEM analysis was used to examine the distribution of PPB in the PLA matrix. Prior to imaging, the samples were gold sputtered for 120 s under vacuum. To produce clear images of the cross-section, imaging was performed utilising a customised sample holder.

### UV-visible Spectrophotometry Analysis

UV-Visible spectrophotometer (SHIMADZU, Japan & Model: UV-3600 plus) was employed to measure the UV-blocking and visible light transparency measurement for PLA and PLA/PPB composite films. The PLA and PLA/PPB composite films were analysed in the wavelength range of 200–700 nm.

### Mechanical Analysis

Universal testing machine (Tinius Olsen, USA and Model: H5K) was used to evaluate the mechanical characteristics like tensile strength (TS) and elongation-at-break (EB %) for PLA and PLA/PPB composite films. ASTM D882 standard was followed for sample preparation and measurements. The cross-head speed was kept at 20 mm/min, and the grip separation was kept at 20 mm. The dimension of the sample used for analysis was fixed to be  $20 \times 10 \times 0.05 \text{ mm}$ . The measurement was carried out in triplicate runs for each sample and the mean values were reported.

### Oxygen Transmission Rate (OTR) Analysis

Gas permeability tester (M/S Labthink, China & model: PERME VAC-VBS) was used in order to obtain information about oxygen permeation characteristics of PLA and PLA/PPB composite films. The ASTM D1434 standard was adopted, and the proportional mode was used. During the analysis, temperature and relative humidity were maintained to be  $30^\circ \text{C}$  and 50%, respectively. For  $\text{O}_2$ , an inlet pressure of 5 bar was set, and the test regime ranged from 0.1 to  $100,000 \text{ cm}^3/\text{m}^3$  for 24 h. 0.1 MPa. The average OTR value was obtained from the analyser directly by performing triplicate analysis for each sample.

### Antioxidant Activity

The free radical scavenging activity (RSA) of PLA and PLA/PPB composite films was determined using 2, 2-diphenyl-1-picrylhydrazyl (DPPH). The sample was incubated for 24 h by immersing ~100 mg of PLA and PLA/PPB composite films in 10 mL of DPPH/methanol solution [20]. The control solution was made with pure DPPH. After incubation, absorbance (at 517 nm) was measured with a UV-Visible spectrophotometer (SHIMADZU, Japan, Model: UV-3600 plus). The following formula (2) was used to corroborate the antioxidant activity of the samples.

$$RSA(\%) = \left[ \frac{(A_c - A_s)}{A_c} \right] \times 100 \quad (2)$$

where,  $A_c$  and  $A_s$  corresponds to absorbance readings for control and test film DPPH solution, respectively. For each sample, the antioxidant activity was evaluated in triplicate runs.

### Antibacterial Studies

The antibacterial activity of PLA and PLA/PPB composites was evaluated using a modified turbidity assay method, as

described by Zhang et al., 2014 [21]. The bacterial suspensions based on Gram-positive *S. aureus* and Gram-negative *E. coli* were prepared with the concentration of  $\sim 10^5$ – $10^6$  CFU/mL. About 200 mg of PLA and PLA/PPB films were added to the bacteria-containing Luria Broth (LB) medium [1.0 g tryptone, 0.5 g yeast extract powder, 1 g NaCl mixed in 100 mL deionized water]. The suspension was incubated at 37 °C with gentle shaking (200 rpm). The optical density (OD600) of the samples at 600 nm was measured every 3 h over a period of 12 h. The bacterial activity of test films as compared to control was reported.

### Migration Analysis

Migration studies for PLA and PLA/PPB composite films were performed in accordance with EU FCM Regulation (EU) 10/2011, using Tenax as a dry food simulant [22]. The PLA and PLA/PPB composite film samples were cut to 20 mm in diameter and sandwiched between 40 mg of Tenax on each side. The samples were then placed in a clean petri dish and heated at 70 °C for 2 h. Following this, samples were weighed to determine the overall migration of PPB into Tenax. For the migration analysis, the following Eq. (3) was utilized.

$$M = \left[ \frac{(m_o - m_f)}{S} \right] \times 1000 \quad (3)$$

where ‘ $M$ ’ corresponds to overall migration ( $\text{mg}/\text{dm}^2$ ),  $m_o$  (mg) and  $m_f$  (mg) corresponds to the initial and final mass of Tenax, respectively. ‘ $S$ ’ represents the surface area of composite films ( $\text{dm}^2$ ). For each sample, measurements were taken in triplicate runs.

### Propylparaben Release Test

The propylparaben release test for PLA/PPB composite films was performed according to the procedure published by Roy and Rhim et al. [20]. Test samples ( $2.5 \times 2.5$  cm) were incubated for 24 h at 37 °C in a conical flask containing 20 mL of distilled water. At regular intervals (0, 24, 48, 72, and 96 h), the absorbance at 420 nm was determined using 2 mL of the collected solution and data was recorded using a UV–Visible spectrophotometer (SHIMADZU, Japan & Model: UV-3600 plus). The amount of PPB release was determined as  $\mu\text{g}$  PPB/ $\text{mm}^2$  of film using a standard curve.

### Statistical Analysis

The mean  $\pm$  standard deviation (S.D.) was reported for all analyses performed in triplicate runs. For the statistical analysis, GraphPad prism® version 7.0 software was used. To examine the statistical significance of the data, the one-way ANOVA test was utilised. \* $p$  0.05, \*\* $p$  0.01, \*\*\* $p$  0.001, and \*\*\*\* $p$  0.0001 were judged significant (when  $n = 3$ ). Values with \* $p < 0.05$ , \*\* $p < 0.01$ , \*\*\* $p < 0.001$  and \*\*\*\* $p < 0.0001$  were thought out as significant (where,  $n = 3$ ).

## Results and Discussion

### TGA

The thermal degradation profile for PPB and PLA/PPB composites are presented in Fig. 1. In Fig. 1a, it can be noticed that the degradation of PPB occurs in the temperature regime of 150–240 °C. In this region,  $\sim 95\%$  of weight loss is recorded for PPB. The thermal analysis results obtained

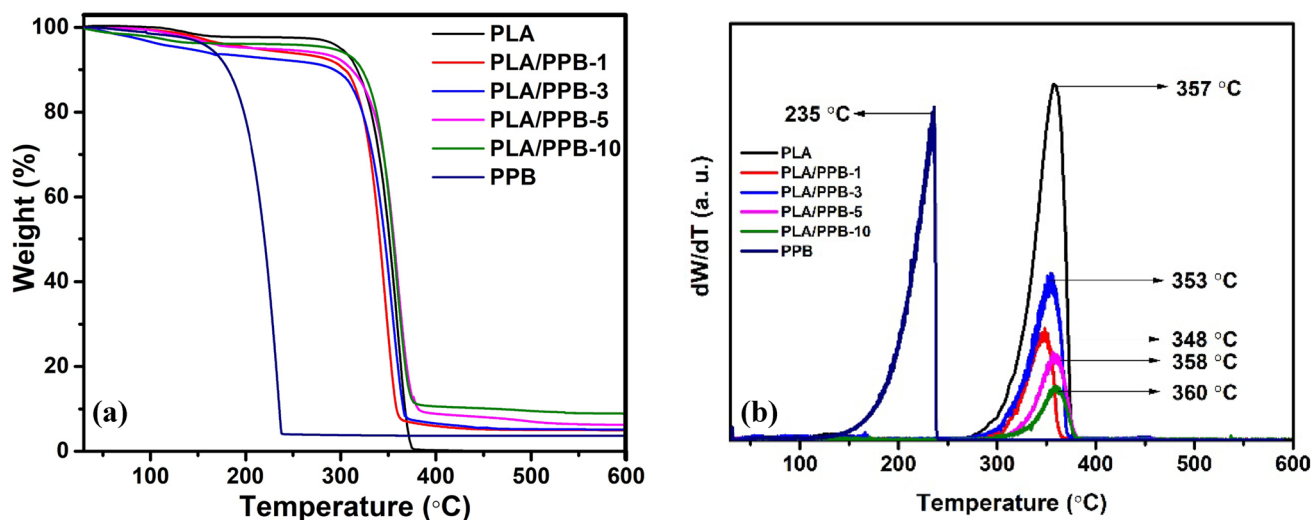


Fig. 1 a TGA and b DTG curves for PPB, PLA and PLA/PPB composites

**Table 1** TGA results for PPB, PLA and PLA/PPB composites

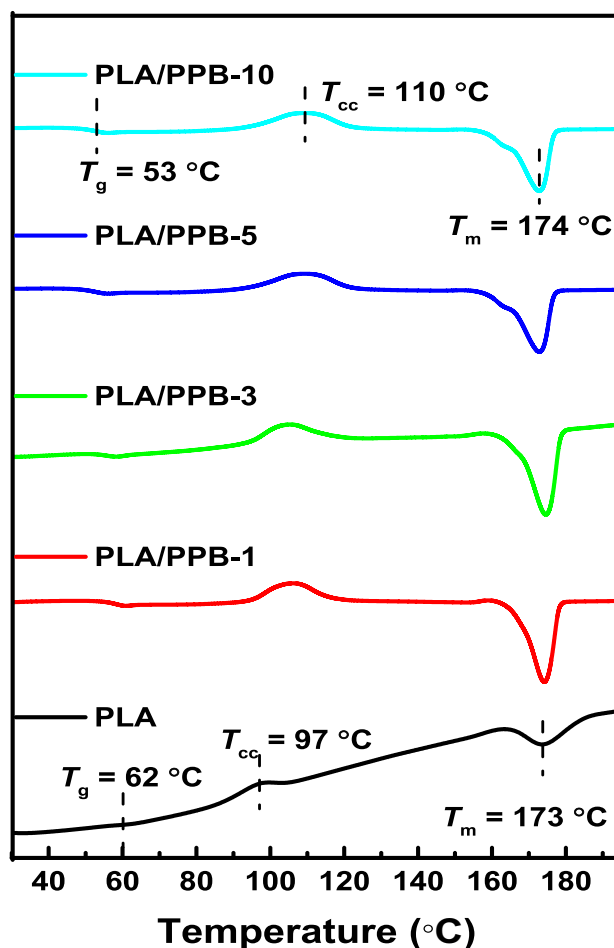
Samples	$T_{10\%}$ (°C)	$T_{50\%}$ (°C)	$T_{max}$ (°C)	Residue (%)
PPB	180	219	235	3
PLA	317	351	357	0.3
PLA/PPB-1	303	341	348	5
PLA/PPB-3	304	346	353	6
PLA/PPB-5	321	354	358	9
PLA/PPB-10	323	355	360	10

for PPB also revealed the formation of char residue, which corresponds to 4 wt%. It can be seen from Fig. 1a that the PLA undergoes two stage degradation process. The first stage of degradation (below 120 °C) is mainly due to the loss of absorbed moisture. The second stage of degradation (300–380 °C) is associated to the breaking up of the PLA backbone via trans-esterification reaction [23].

The PLA/PPB composites also undergo double stage degradation process like PLA. In order to understand the thermal degradation behaviour of PLA/PPB composites,  $T_{onset}$  (thermal decomposition when 10% weight loss occurs),  $T_{50\%}$  (temperature at which 50% weight loss occurs) and  $T_{max}$  (temperature at which maximum degradation occurs) are derived from the thermal degradation profile and presented in Table 1. It can be observed from Table 1 that the PLA exhibits  $T_{onset}$  at 317 °C. The  $T_{onset}$ ,  $T_{50\%}$  and  $T_{max}$  for PLA/PPB composites tends to decrease till 3 wt% loadings of PPB in the PLA matrix. With further increase in the wt% loadings (5 and 10 wt%) of PPB in the PLA matrix, the thermal stability of the composites is observed to shoot up. This may be associated with the formation of char residue in the case of PLA/PPB (5 and 10 wt%) composites. This may be due to the formation of thermally resistive char on the surface of PLA/PPB composites. This in turn leads to the protection of bulk material during the thermal degradation process. Similar results have been reported by Liu et al. in which the increase in wt% of filler concentration led to an increase in the wt% of thermally resistive char formation [24].

### DSC Analysis

The DSC thermographs for PLA and PLA/PPB composites obtained during the second heating cycle are shown in Fig. 2 and the values for thermal characteristics are summarized in Table 2. From Table 2, it can be observed that the glass transition temperature ( $T_g$ ) for PLA occurs at 62 °C. The  $T_g$  of the PLA/PPB composites show gradual reduction with respect to wt% loadings of PPB in PLA

**Fig. 2** DSC thermographs for PLA and PLA/PPB composites

matrix. The decline in  $T_g$  observed for the composites can be attributed to the plasticizing impact of PPB in the PLA matrix. The cold crystallization ( $T_{cc}$ ) for PLA film is recorded at 97.5 °C, while PLA/PPB composites exhibit increase in the  $T_{cc}$  with respect to wt% loadings of PPB. The decrement in the intensity and widening of  $T_{cc}$  peak for PLA/PPB composites is observed with increase in the wt% of PPB in the PLA matrix. This indicates slower crystallisation process for PLA in the presence of PPB additive. It can be seen from Table 2, that PLA/PPB composites demonstrate an increase in the % crystallinity (10.9 to 18.7%) in comparison with PLA. The PLA/PPB-3 and PLA/PPB-5 exhibit slight decrease in the % $X_c$  followed by PLA/PPB-1 composite. Among all the composites, PLA/PPB-10 records the lowest % $X_c$  value. The shift in  $T_{cc}$  towards higher temperature side observed for all the PLA/PPB composites and decrement in % $X_c$  w.r.t wt% loadings

**Table 2** DSC results for PLA and PLA/PPB composites

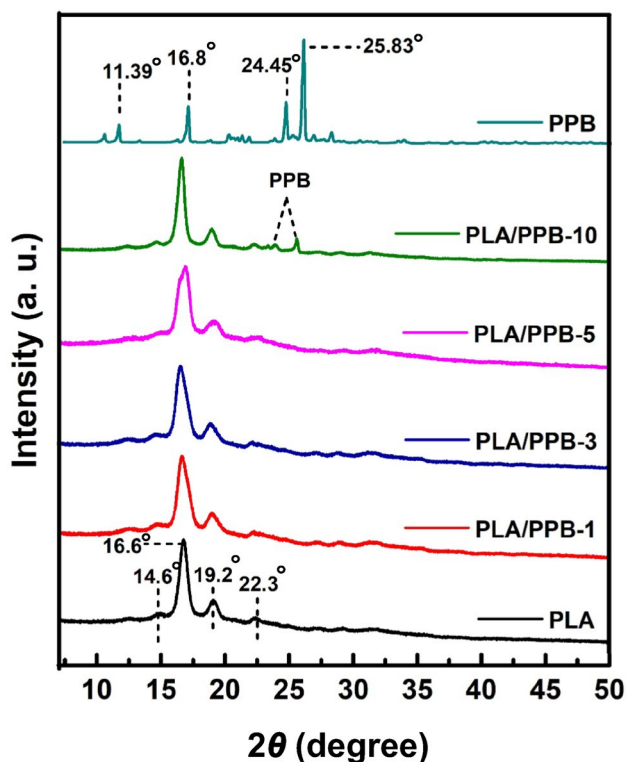
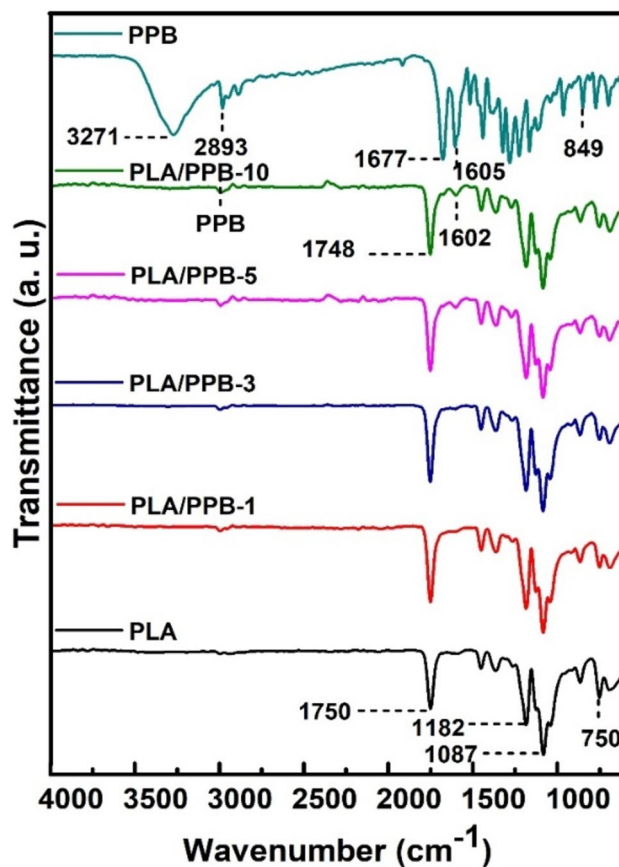
Samples	$T_g$ (°C)	$T_{cc}$ (°C)	$T_m$ (°C)	$\Delta H_{cc}$	$\Delta H_m$	% $X_c$
PLA	62	97.5	173	5.26	15.40	10.9
PLA/PPB-1	56	106	173	36.58	19.04	18.74
PLA/PPB-3	56	106	174	41.77	25.63	17.24
PLA/PPB-5	53	109	174	42.66	26.79	16.94
PLA/PPB-10	53	110	174	21.09	16.23	13.73

of PPB correspond to slower diffusion rate of PLA towards the surface of the nucleus during crystallization process. The  $T_m$  for PLA occurs at 173 °C, while the PLA/PPB-1, PLA/PPB-5 and PLA/PPB-10 composite registers  $T_m$  at 173 °C, 174 °C and 174 °C, respectively.

### XRD Analysis

The XRD pattern for PLA and PLA/PPB composite films are shown in Fig. 3. The XRD pattern obtained for PPB is identical with the JCPDS file [25]. It can be observed from Figure 3 that the PLA presents a dominant peak at  $2\theta = 16.8^\circ$ , which is attributed to the reflections obtained from (1 1 0)/(2 0 0) planes and confirms the orthorhombic  $\alpha$ -crystalline phase. The less intense peaks which appear at  $2\theta = 14.9^\circ$ ,  $19.2^\circ$  and  $22.6^\circ$  are attributed to the reflections obtained from (0 1 0), (2 0 3) and (2 1 0) planes, respectively. This in turn

confirms the  $\alpha$ -phase of PLA biopolymer. The XRD pattern obtained for neat PLA represents the  $\alpha$ -crystalline structure [23, 26]. The PLA/PPB composites show predominant peak for PLA at  $2\theta = 16.8^\circ$ , and this remains unchanged which indicates that the lattice parameters as well as overall crystal structure are not significantly affected by presence of PPB. Further, the PLA/PPB-10 composite exhibits two additional peaks at  $2\theta = 24.4^\circ$  and  $25.8^\circ$ , which corresponds to the presence of PPB in the PLA matrix. In the case of other PLA composites, the characteristic peaks representing PPB are missing. This may be due to the lower wt.% loadings of PPB in the PLA matrix.

**Fig. 3** XRD pattern for PPB, PLA and PLA/PPB composites**Fig. 4** FTIR spectra for PPB, PLA and PLA/PPB composites

## FTIR Analysis

The FTIR spectra for PPB, PLA and PLA/PPB composites are shown in Fig. 4. In the case of PPB, broad peak observed at  $3271\text{ cm}^{-1}$  is attributed to O–H stretching. The characteristic peaks recorded at  $2980$  and  $2893\text{ cm}^{-1}$  are associated with asymmetric and symmetric C–H stretching of methyl groups. The peak at  $1677\text{ cm}^{-1}$  can be attributed to the stretching of C=O functional group. The peaks observed at  $1280$  and  $1224\text{ cm}^{-1}$  correspond to the presence of C–O stretching [27]. It is also clear from Fig. 4 that the characteristic peak for PLA appears at  $1750\text{ cm}^{-1}$  which corresponds to the stretching of ester group in backbone of PLA [28]. The peak observed at  $1450\text{ cm}^{-1}$  is associated to the bending of methyl groups in PLA. The asymmetric bending of –CH– groups in PLA correlates to the occurrence of band position at  $1361\text{ cm}^{-1}$ . The presence of peak at  $1182\text{ cm}^{-1}$  relates to the asymmetric stretching of –C–O–C. The peaks at  $1087$  and  $866\text{ cm}^{-1}$  are associated

with the stretching behaviour of –C–O and –C–C functional groups of PLA [29]. Furthermore, an additional peak that appears at  $750\text{ cm}^{-1}$  corresponds to –C–C– stretching in the semi-crystalline phase of PLA biopolymer [30]. All the characteristic peaks of PLA can be evidenced for PLA/PPB composites. The predominant characteristic peak of PLA observed at  $1750\text{ cm}^{-1}$  is shifted to a lower wavelength  $1748\text{ cm}^{-1}$  and the intensity of the peak is reduced for PLA/PPB composites. The shift towards a lower wavelength might be possible due to the interaction between C=O group in the ester linkage of PLA and the hydroxyl group of propylparaben [31]. Furthermore, PLA/PPB composite has a small peak at  $1602\text{ cm}^{-1}$  which corresponds to the C=C aromatic stretching of PPB.

## Morphology

The surface morphology of PPB, PLA and PLA/PPB composite films were observed using FE-SEM analysis and their

**Fig. 5** FE-SEM images of a surface morphology b) cross-section morphology for PLA and PLA/PPB composites

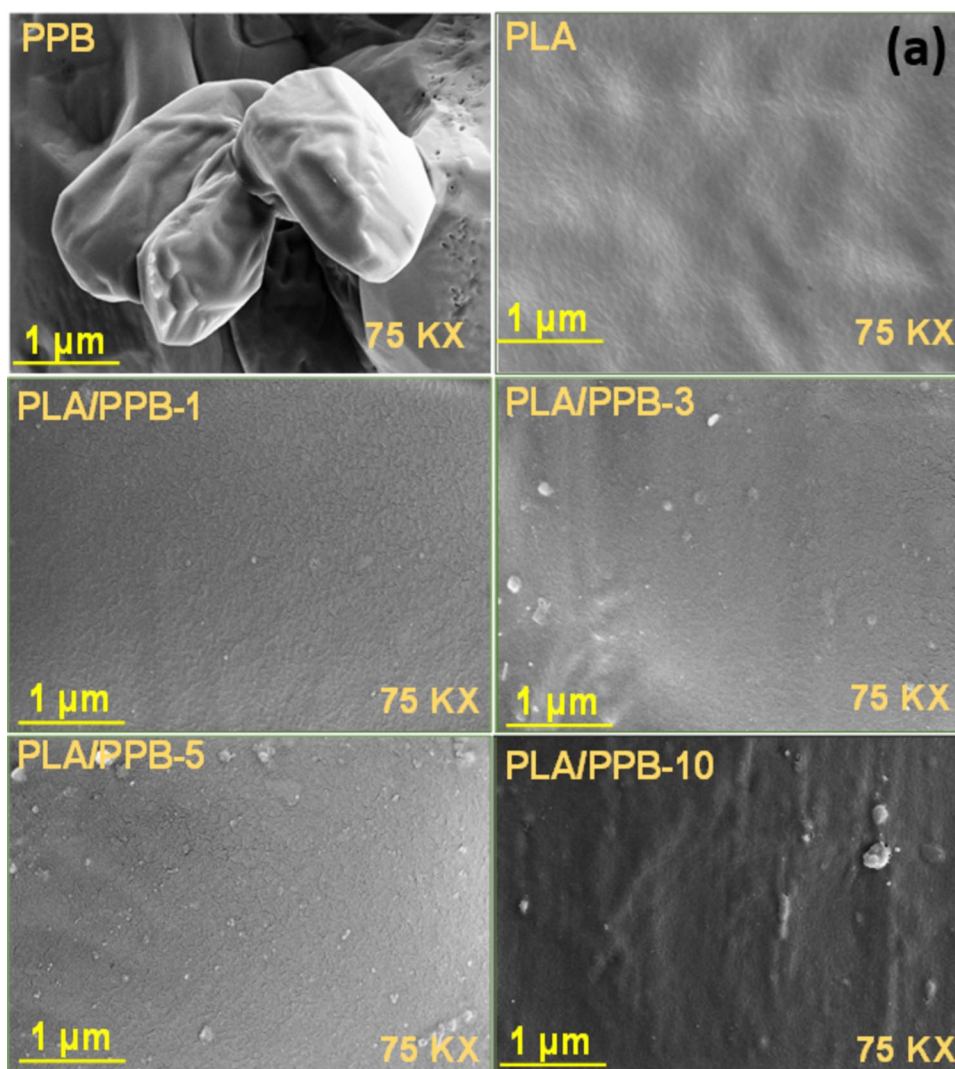
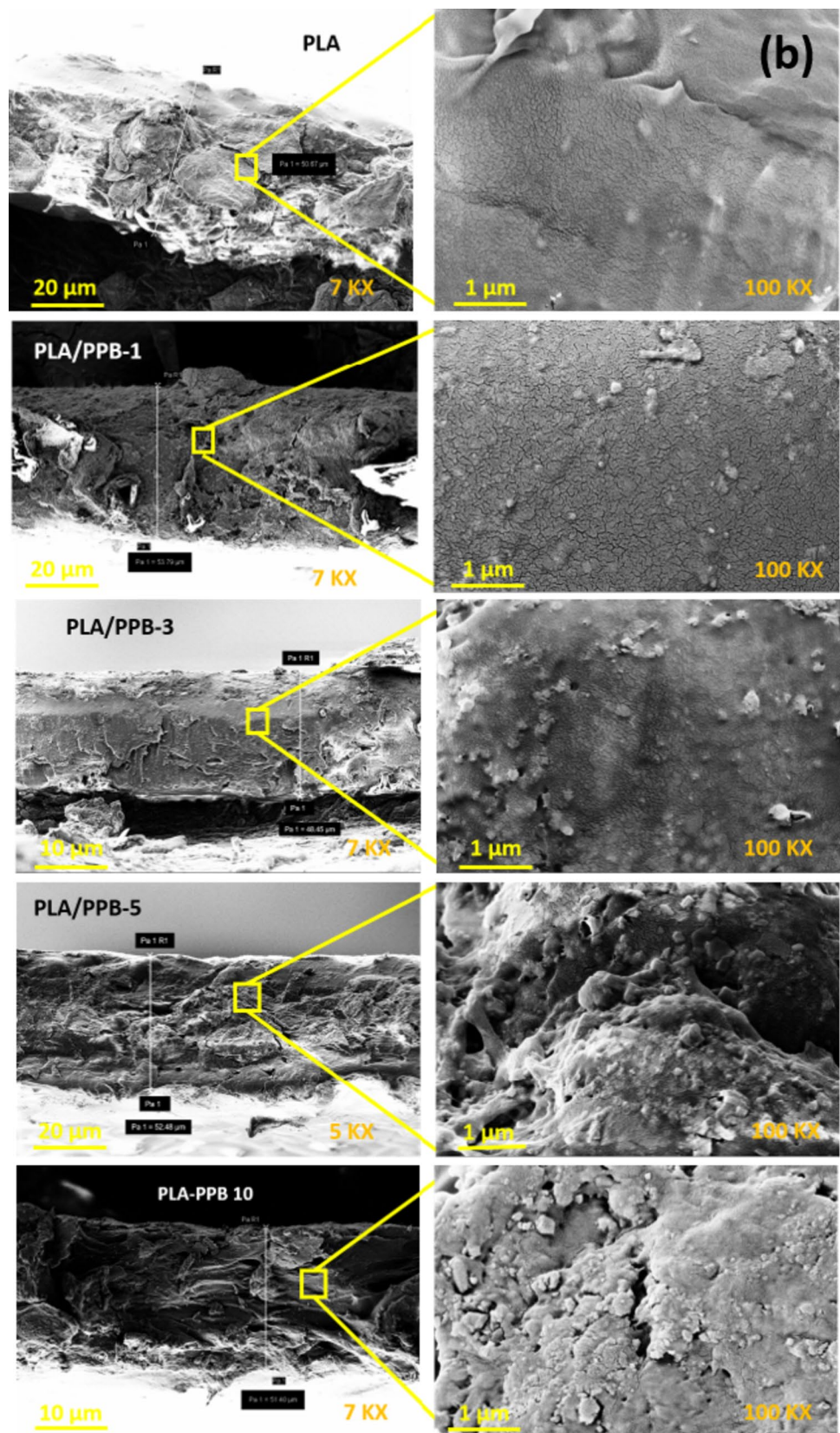




Fig. 5 (continued)



**Table 3** UV and Visible light analysis results for PLA and PLA/PPB composites films

Samples	UV @ 320 nm (Blockage)	Visible @ 660 nm (Trans- parency)
PLA	48	81
PLA/PPB-1	60	47
PLA/PPB-3	58	43
PLA/PPB-5	70	40
PLA/PPB-10	85	30

representative images are shown in Fig. 5. The morphology of PPB resembles like a bean shaped structure. In the case of PLA, the surface of the film seems to be smooth and free from cavities. Similar, observations were made from the cross-section morphology images as well. The presence of PPB in the PLA matrix is evident from the FE-SEM morphology of PLA/PPB composites. In the case of PLA/PPB-10, agglomeration could be visible, which may be due to higher wt% loadings. The SEM analysis clearly shows that as the wt% loading of PPB increases in the film, there is more agglomeration and aggregation of the filler within the polymer matrix.

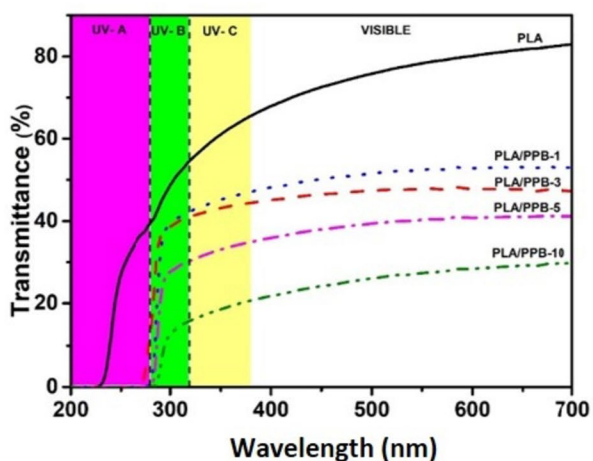
### Transparency Analysis

The UV–Visible and contact transparency images for PLA and PLA/PPB composites are shown in Fig. 6. The UV–visible transmission is an important parameter to be considered for prospective packaging material. In general, UV blockage property is necessary to avoid discoloration, nutrient loss and UV degradation [32]. Likewise, high visible transparency is also important to be achieved for see

through packaging. It can be seen from Fig. 6a that the PLA seems to block ~40% UV–B light at  $\lambda = 280$  nm and transmit ~82% of visible light at  $\lambda = 700$  nm. In comparison with PLA, the PLA/PPB composites show an increment in UV blocking characterization and reduction in visible light transmission. It can be seen from the Fig. 6a that the PLA/PPB-10 composite exhibits ~85% UV–B blockage at  $\lambda = 320$  nm. However, the highest UV–B blockage demonstrated by PLA/PPB-10 is at the expense of significant reduction in visible light transmission at  $\lambda = 660$  nm. Therefore, PLA/PPB-5 composite seems to be promising for food packaging application, as it exhibits ~70% of UV-B blockage and allows ~40% transmission of visible light. Further, it can be observed from Fig. 6b that the PLA/PPB composites show similar contact transparency like neat PLA (Table 3).

### Mechanical Properties

The tensile strength (TS), elongation at break (EB) and Young's modulus (EM) obtained for PLA and PLA/PPB composites are shown in Fig. 7. The TS of PLA is recorded at 26 MPa, while the composites demonstrate slightly better performance. The tensile strength of PLA/PPB-1 is recorded at 42 MPa, which is the highest among all the composites. The PLA/PPB-3 exhibits a slight decrease in TS (38 MPa) which is closely followed by PLA/PPB-5 (39 MPa), respectively. The least improvement in TS (32 MPa) is noticed for PLA/PPB-10 compared to neat PLA. However, all the PPB composites exhibit increasing in TS, which might be due to the interaction between the C=O group in the ester linkage of PLA and the hydroxyl group of propylparaben as shown in the FTIR analysis. The EB (flexibility) is a key feature to evaluate the viability of any polymer composites in the food packaging industry [33]. The EB value for PLA is 3.2%, which shows PLA is brittle, and inflexible making it difficult to be

**Fig. 6** a UV–Visible light transmission analysis and b contact transparency images for PLA and PLA/PPB composites

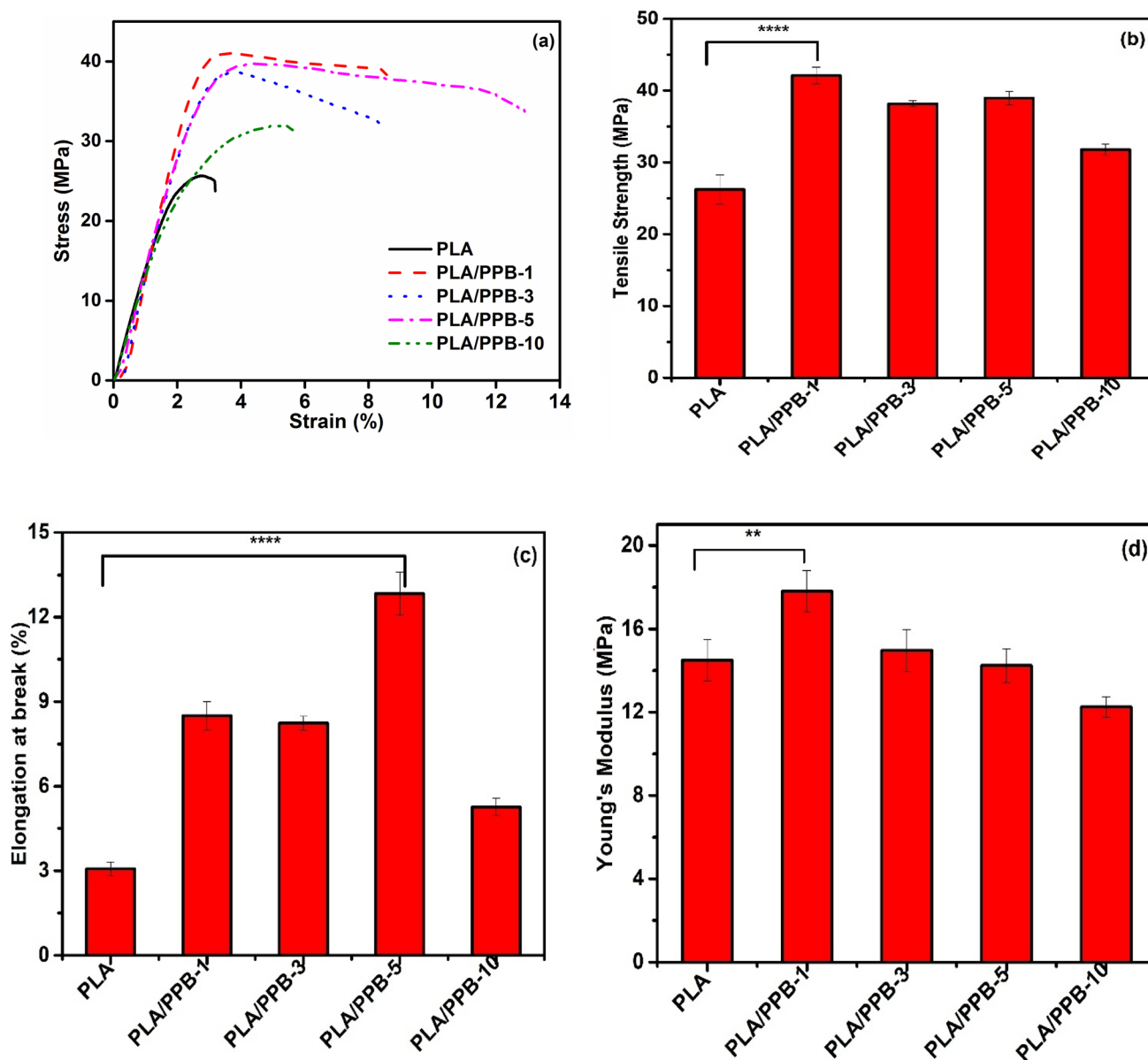


**Fig. 7** a stress-strain curve, b tensile strength, c elongation at break and d Young's modulus for PLA and PLA/PPB composite films. [ $p < 0.05$ ,  $**p < 0.01$ ,  $***p < 0.001$  and  $****p < 0.0001$  (one-way ANOVA)]

employed in the food packaging industry. The presence of PPB in the PLA matrix significantly improved the EB value. The EB values for PLA/PPB-1 and PLA/PPB-3 are recorded at 8.5% as compared to PLA. Among all the composites, PLA/PPB-5 exhibits the highest EB value (12.8%), which is an almost four-fold increase as compared to PLA with a significant increase of ( $p < 0.0001$ ). Further, PLA/PPB-10 composites show drastic reduction in EB%, which might be due to increased agglomeration at higher wt% loadings. This indicates that the incorporation of PPB in the PLA matrix significantly improved its flexibility while reducing its brittleness. The best performance in terms of Young's modulus

is exhibited by PLA/PPB-1 composite with the significance of ( $P < 0.01$ ), which is then closely followed by PLA/PPB-3 and PLA/PPB-5 in comparison with neat PLA. Among all the samples, PLA/PPB-10 records the lowest Young's modulus value than PLA films. These results indicate that the composites at lower wt% loading of PPB can withstand more stretching pressure without deforming unlike PLA.

### Oxygen Transmission Rate (OTR) Analysis

The OTR is an important parameter required for food packaging films in order to prevent the food from oxidative

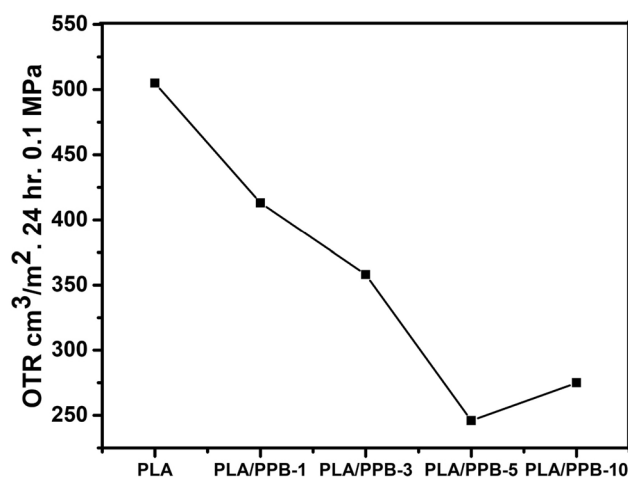


**Fig. 8** Oxygen transmission rate analysis for PLA and PLA/PPB composites

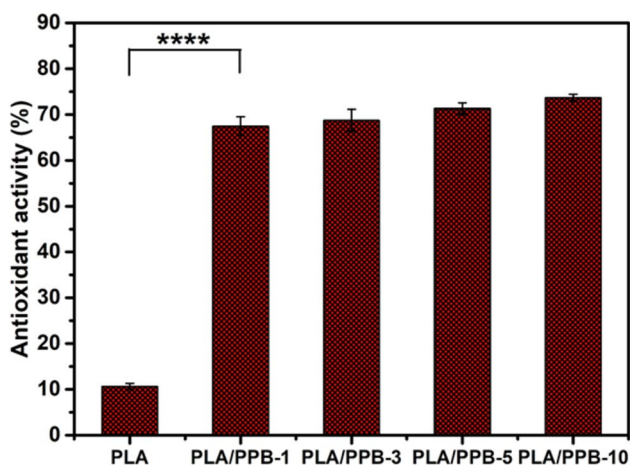


**Fig. 9** Antioxidant activity for PLA and PLA/PPB composite films. [ $*p < 0.05$ ,  $**p < 0.01$ ,  $***p < 0.001$  and  $****p < 0.0001$  (one-way ANOVA)]

spoilage. Reduction in OTR helps in prevention of transmission from external environment through the films, such that shelf-life of stored food can be extended. Figure 8 shows the oxygen transmission rate (OTR) property for PLA and PLA/PPB composites. It can be seen from Fig. 8 that PLA exhibits the highest permeation of  $O_2$  through the film, which indicates its poor  $O_2$  barrier property. The addition of PPB in the PLA matrix seems to achieve reduction in  $O_2$  permeation through the films. The maximum reduction in  $O_2$  permeation is exhibited by PLA/PPB-5 composites in comparison with PLA. The reduction in OTR is associated with tortuous path effect created by the presence of PPB in the PLA matrix. At higher wt% loadings (10 wt%) of PPB in the PLA matrix, the OTR tends to slightly increase, which may be due to the agglomeration phenomenon. Yu et al., 2021, developed a

PLA based composite film reinforced with acetylated cellulose nanocrystals and ZnO for active food packaging application. Notably, PLA/ACNC/5%ZnO composite exhibits a 43% decrease in the OTR. Similarly, PLA/PPB-5 composite demonstrates a 50% decrease in the OTR property which is more suitable for the active food packaging application [31].

### Antioxidant Activity

Antioxidant activity is an important property required for packaging films in order to prevent the food from spoilage due to oxidation process. The antioxidant activity of PLA and PLA/PPB composite films were measured using the DPPH radical scavenging activity, and the results are shown in Fig. 9. The antioxidant activity of PLA seems to be significantly higher with respect to the addition of PPB in PLA matrix. The antioxidant activity exhibited by PLA/PPB composites fall in the range of 67–73%. The antioxidant activity of PPB can be attributed to the donation of hydrogen atom present in the phenolic group of PPB. Similar phenomenon has been reported by PLA/Curcumin composite film for active packaging films [20]. The improvement in terms of anti-oxidant activity exhibited by PLA/PPB composite suggests that this formulation could be effective for packaging food products that are susceptible to oxidative stress during storage. Yang et al. [34], recently developed PLA/ethylenevinylacetate-glycidyl methacrylate (NPG)/1LMP (lignin microparticles) with high antioxidant properties (RSA 81%) [34]. The PLA/PPB composites developed in the current work also exhibits similar results in terms of antioxidant properties.

### Antibacterial Activity

The antibacterial activity for PLA and PLA/PPB films were assessed using turbidity assay and the results are presented in Fig. 10. It can be seen from Fig. 10 that the PLA exhibits similar OD value like the control, which indicates the lack of antibacterial activity in PLA. It was observed that incorporation of PPB in the PLA matrix hinders the growth rate for bacteria in the suspension. The PLA/PPB-1 composite shows slightly better antibacterial activity in both *E. coli* and *S. aureus* suspensions in comparison with the control sample. The antibacterial activity increases with the wt% loadings of PPB incorporated in the PLA matrix. As compared to control and PLA, PLA/PPB-5 and PLA/PPB-10 exhibits drastic increase in anti-bacterial activity (52 and 75%, respectively). The antibacterial activity of PPB is due to the alteration of cell membrane properties through potassium efflux which is aligned to the porin expression in the membrane of the bacterial target, thereby hindering growth and multiplication [18].

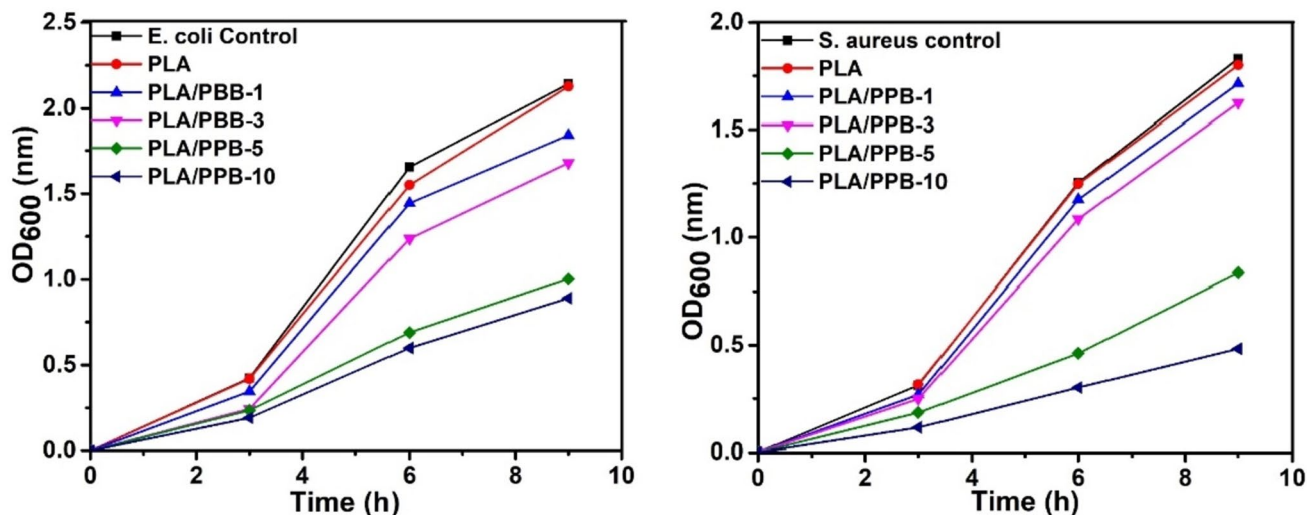


Fig. 10 Antibacterial activity assessment for PLA/PPB composites using turbidity assay

### Migration Studies

The overall migration (OM) studies for PLA and PLA/PPB composites were carried out using Tenax as dry food simulant. This study was performed to quantify the non-volatile constituent amount present in the films which may migrate during dry food storage and the results are shown in Fig. 11. The migration test was carried out in accordance with the European Union Commission Legislation (EU) No. 10/2011 regulations and the acceptable limit is set to be 10 mg/dm<sup>2</sup>. It can be seen from Fig. 11 that the PLA records the least migration of ~2 mg/dm<sup>2</sup>. On the other hand, the overall migration value for PLA/PPB composites is found to be in the range of 2–9 mg/dm<sup>2</sup>. The OM values obtained for all the PLA/PPB composites

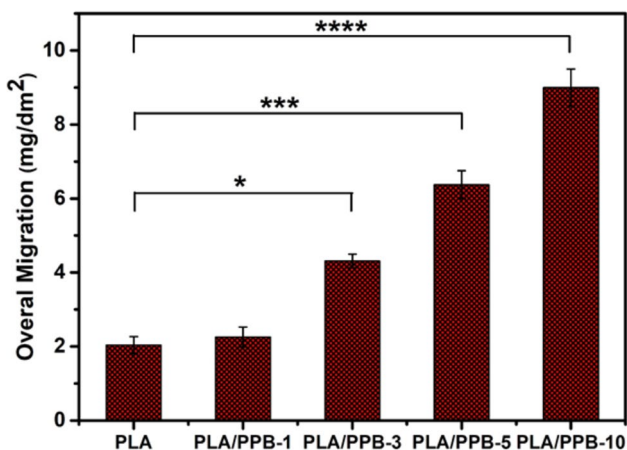


Fig. 11 Migration analysis for PLA and PLA/PPB composite films using tenax as dry food simulant. [ $*p < 0.05$ ,  $**p < 0.01$ ,  $***p < 0.001$  and  $****p < 0.0001$  (one-way ANOVA)]

films fall below the limit set by (EU) No. 10/2011 regulations, which suggest their suitability for dry food packaging application.

### Propylparaben Release Test

The propyl paraben release profile for PLA/PPB composites are shown in Fig. 12. In the beginning, the release was found to be slower and not noticeable. It can be seen from Fig. 12 that increasing trend in release profile is observed with respect to wt% loadings of PPB in the PLA matrix throughout the analysis period (4 days). The slowest release (3.0  $\mu\text{g}/\text{mm}^2$ ) is exhibited by PLA/PPB-1 whereas the PLA/PPB-10 composite is found to exhibit the highest release (5.6

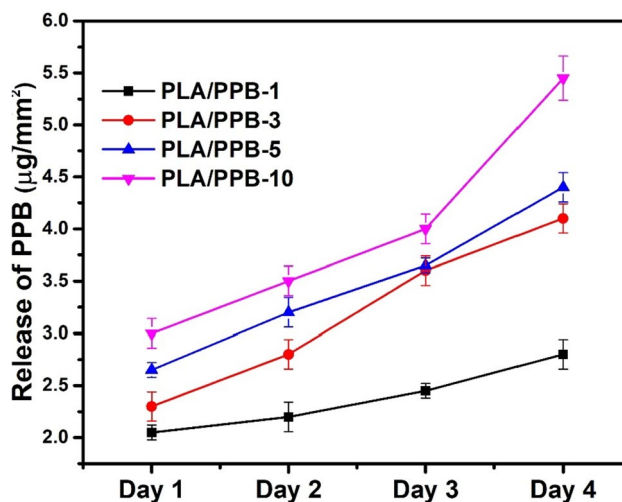


Fig. 12 Propylparaben release profile for PLA/PPB composites films. [ $*p < 0.05$ ,  $**p < 0.01$ ,  $***p < 0.001$  and  $****p < 0.0001$  (one-way ANOVA)]

$\mu\text{g}/\text{mm}^2$ ) throughout the analysis period. The slow release of PPB can be attributed to the poor water solubility of PLA in the first instance and also the low solubility of PPB in water which limits its diffusion into the distilled water medium. The pore structures of polymer matrixes and their solubility in water are important factors in the nature of release of bioactive fillers from their composites [35, 36].

## Conclusions

In the current work, propylparaben “PPB” is used as an additive in the PLA matrix and its active food packaging characteristics are envisaged. The incorporation of PPB in the PLA matrix shows reduction in the  $T_{\text{max}}$  value as compared to PLA film. From the DSC analysis, increment in the  $T_{\text{cc}}$  value for PLA/PPB composite reveals that the presence of PPB in the PLA matrix suppresses the diffusion rate of PLA chains to the surface of the nucleus and hence slows down the rate of crystallization process. The PLA/PPB-5 composite films showed 70% blockage of UV-B light at 320 nm while maintaining 40% transparency at 660 nm. The reinforcement of 5 wt% loading of PPB in the PLA matrix significantly improved the elongation-at-break by almost four-fold increase with a significance of ( $p < 0.0001$ ) in comparison with PLA film. The PLA/PPB composite films are found to be effective in controlling the growth of food borne pathogenic bacteria (*E. coli* and *S. aureus*). The PLA/PPB composites have shown significant improvement (70%) in the DPPH scavenging activity with significance of ( $p < 0.0001$ ). The migration analysis carried out for PLA/PPB composites revealed that the quantified OM values are found to be within the set limit of  $10 \text{ mg}/\text{dm}^2$  as per EU regulation. The PLA/PPB-5 composite film shows promising feature in terms of UV-blockage, antioxidant property, enhanced ductility, as well as antibacterial characteristics, and therefore can find potential application as active food packaging material.

**Acknowledgements** The authors sincerely thanks Council of Scientific and Industrial Research (CSIR), India and The World Academy of Science (TWAS), Italy for post graduate fellowship (Grant No: 22/FF/CSIR-TWAS/2018) to carryout doctoral research at CSIR-CECRI, India. The corresponding author “Ravi Babu Valapa” sincerely thanks SERB, DST for financial support under EMEQ scheme (Grant: no: EEQ/2019/000451) and CSIR-HQ for funding under “AEISS theme” (Grant no: MLP 0318). Sravanthi Loganathan sincerely thanks Department of Science and Technology, Govt. of India for funding this research under DST INSPIRE FACULTY Scheme (Grant no: DST/INSPIRE/04/2017/000704). All the authors acknowledge Central Instrumentation Facility (CIF) at CSIR-CECRI for providing characterization facilities.

**Author Contributions** UL: experiments, characterization, data collection, formal analysis, validation, and preparation of original draft. VR: characterization, analysis, writeup—review and editing. AG:

characterization, analysis, writeup—review and editing. SL: resources and writeup—review and editing. RBV: Conceptualization, supervision, resources, writeup—review and editing and funding acquisition.

## Declarations

**Competing Interests** The authors declare no competing interests.

## References

- Jia-hui Wu Teng-gen, Hu H, Wang Min-hua, Zong H, Wu, Wen P (2022) Electrospinning of PLA nanofibers: recent advances and its potential application for Food Packaging. *J Agric Food Chem* 70(27):8207–8221. <https://doi.org/10.1021/acs.jafc.2c02611>
- Halimatul MJ, Sapuan SM, Jawaid M, Ishak MR, Ilyas RA (2019) Effect of sago starch and plasticizer content on the properties of thermoplastic films: mechanical testing and cyclic soaking-drying. *Polimery* 64:32–41. <https://doi.org/10.14314/polimery.2019.6.5>
- Dorgan JR, Lehermeier HJ, Palade L-I, Cicero J (2001) Poly-lactides: properties and prospects of an environmentally benign plastic from renewable resources. *Macromol Symp* 175:55–66
- Daniela C, Gonzalo B, Carolina V, Nicolás B, Giannina AT, María PG, Francisco R, Adrián R, María JG, Luis C, Mauricio Y, Julio R, Alejandra T (2021) Effect of supercritical incorporation of cinnamaldehyde on physical-chemical properties, disintegration and toxicity studies of PLA/lignin nanocomposites. *Int J Biol Macromol* 167:255–266
- Xipo Z, Jinchao L, Juncheng L, Xinyu L, Weiyei Z, Shaoxian P (2022) Strategies and techniques for improving heat resistance and mechanical performances of poly (lactic acid) (PLA) biodegradable materials. *Int J Biol Macromol* 218:115–134
- Lawal U, Ravi Babu V (2021) Bioplastics: an introduction to the role of Eco-friendly Alternative Plastics in sustainable packaging. In: Sapuan SM, Ilyas RA (eds) *Bio-based Packaging: material, Environmental and Economic aspects*. John Wiley & Sons, Inc., New Jersey, pp 319–334
- Mulla MZ, Rahman MRT, Marcos B, Tiwari B, Pathania S (2021) Poly lactic acid (PLA) nanocomposites: Effect of Inorganic nanoparticles reinforcement on its performance and food packaging applications. *Molecules* 26:1967. <https://doi.org/10.3390/molecules26071967>
- Panitee Suwanamornlert N, Kerddonfag A, Sane W, Chinsirikul W, Zhou V, Chonhenchob (2020) Poly(lactic acid)/poly(butylene-succinate-co-adipate) (PLA/PBSA) blend films containing thymol as alternative to synthetic preservatives for active packaging of bread. *Food Packag Shelf Life* 25:100515. <https://doi.org/10.1016/j.fpsl.2020.100515>
- Santos X, Álvarez M, Videira-Quintela D, Mediero A, Rodríguez J, Guillén F, Pozuelo J, Martín O (2022) Antibacterial capability of MXene (Ti3C2Tx) to produce PLA active contact surfaces for Food Packaging Applications. *Membranes* 12:1146. <https://doi.org/10.3390/membranes12111146>
- Guillen DV-QF, Martin O, Cumbal L, Montalvo G (2022) Antibacterial and antioxidant triple-side filler composed of fumed silica, iron, and tea polyphenols for active food packaging. *Food Control* 138:0956–7135. <https://doi.org/10.1016/j.foodcont.2022.109036>
- Value-Added Biopolymer Nanocomposites from Waste Eggshell-Based CaCO<sub>3</sub> Nanoparticles as Fillers Tarig, Hassan A, Rangari VK, Jeelani S (2014) *ACS Sustain Chem Eng* 2(4):706–717. <https://doi.org/10.1021/sc4004005v>

12. Udangshree Boro A, Priyadarsini VS, Moholkar (2022) Synthesis and characterization of poly(lactic acid)/clove essential oil/alkali-treated halloysite nanotubes composite films for food packaging applications. *Int J Biol Macromol* 216:927–939. <https://doi.org/10.1016/j.ijbiomac.2022.07.209>
13. Mohan Subbuvel P, Kavan (2022) Preparation and characterization of polylactic acid/fenugreek essential oil/curcumin composite films for food packaging applications. *Int J Biol Macromol* 194:470–483. <https://doi.org/10.1016/j.ijbiomac.2021.11.090>
14. Llana-Ruiz-Cabello M, Pichardo S, Bermúdez JM, Baños A, Núñez C, Guillamón E, Aucejo S, Cameán AM (2016) Development of PLA films containing oregano essential oil (*Origanum vulgare* L. Virens) intended for use in food packaging. *Food Addit Contaminants: Part A* 33(8):1374–1386. <https://doi.org/10.1080/19440049.2016.1204666>
15. Cvek M, Paul UC, Athanassiou (2022) Biodegradable Films of PLA/PPC and curcumin as packaging materials and smart Indicators of food spoilage. *ACS Appl Mater Interfaces* 14(12):14654–14667. <https://doi.org/10.1021/acscami.2c02181>
16. Lincho J, Martins RC, Gomes J (2021) Paraben Compounds—Part I: an overview of their characteristics, detection, and impacts. *Appl Sci* 11:2307. <https://doi.org/10.3390/app11052307>
17. Jinbo O, Jian C, Limin Z, Zhirong L, Chuntao Z (2020) Solubility Measurement, modeling, and dissolution thermodynamics of Propylparaben in 12 pure solvents. *J Chem Eng Data* 65:9, 4725–4734
18. Jérôme B, Anne D-R, Jean-Marie P (2005) Propyl paraben induces potassium efflux in *Escherichia coli*. *J Antimicrob Chemother* 55:6, 1013–1015. <https://doi.org/10.1093/jac/dki110>
19. Chung D, Chikindas ML, Yam KL (2001) Inhibition of *Saccharomyces cerevisiae* by slow release of propyl paraben from a polymer coating. *J Food Prot* 64(9):1420–1424
20. Swarup R, Jong-Whan R (2020) Preparation of bioactive functional poly (lactic acid)/curcumin composite film for food packaging application. *Int J Biol Macromol* 162:1780–1789
21. Mei Z, Ping W, Hongyan S, Zuankai W (2014) Superhydrophobic Surface with Hierarchical Architecture and Bimetallic Composition for enhanced antibacterial activity. *ACS Appl Mater Interfaces* 6:22108–22115
22. Evie LP, Uttam CP, Thi NT, Giulia S, Luca C, Sergio M, Richard D, Athanassia A (2019) Sustainable active food packaging from Poly(lactic acid) and Cocoa Bean shells. *ACS Appl Mater Interfaces* 11:34
23. Valapa RB, Pugazhenth G, Katiyar V (2014) Fabrication and characterization of sucrose palmitate reinforced poly (lactic acid) bionanocomposite films. *J Appl Polym Sci* 132:41320. <https://doi.org/10.1002/app.41320>
24. Khalili P, Liu X, Zhao Z, Blinzler B (2019) Fully biodegradable composites: thermal, flammability, moisture absorption and mechanical properties of natural fibre-reinforced composites with nano-hydroxyapatite. *Materials* 12(7):1145
25. JCPDS file no. 00-051-1982
26. Laura A, Patrizia C, Maria BC, Maria CR, Massimo G, Andrea L (2017) Effect of nucleating agents on crystallinity and properties of poly (lactic acid) (PLA). *Eur Polym J* 93:822–832
27. Solanki S, Siva BP, Rajesh N, Suthan T (2017) Growth and characterization of propyl 4-hydroxybenzoate single crystal by vertical Bridgman technique. *Mater Res Innov* 22:144–146. <https://doi.org/10.1080/14328917.2016.1266428>
28. Pracella M, Haque MMU, Puglia D (2014) Morphology and properties tuning of PLA/cellulosenanocrystals bio-nanocomposites by means of reactive functionalization and blending with PVAc. *Polymer* 55:3720–3728
29. Rocca-Smith JR, Lagorce-Tachon A, Iaconelli C, Bellat JP, Marcuzzo E, Sensidoni A, Piasente F, Debeaufort F, Karbowiak T (2017) How high pressure CO<sub>2</sub> impacts PLA film properties. *Expr Polym Lett* 11:320–333
30. Muller J, González C, Chiralt A (2017) Poly(lactic acid) (PLA) and starch bilayer films, containing cinnamaldehyde, obtained by compression moulding. *Eur Polym J* 95:56–70. <https://doi.org/10.1016/j.eurpolymj.2017.07.019>
31. Yu F, Fei X, He Y, Li H (2021) Poly(lactic acid)-based composite film reinforced with acetylated cellulose nanocrystals and ZnO nanoparticles for active food packaging. *Int J Biol Macromol* 186:770–779. <https://doi.org/10.1016/j.ijbiomac.2021.07.09>
32. Cavallo E, He X, Luzi F, Dominici F, Cerrutti P, Bernal C, Foresti ML, Torre L, Puglia D, Protective UV (2020) Antioxidant, Antibacterial and Compostable Poly(lactic acid) composites containing pristine and chemically modified lignin nanoparticles. *Molecules* 26(1):126. <https://doi.org/10.3390/molecules26010126>
33. El-hadi AM (2017) Increase the elongation at break of poly (lactic acid) composites for use in food packaging films. *Sci Rep* 7:46767. <https://doi.org/10.1038/srep46767>
34. Yang W, Weng Y, Puglia D, Qi G, Dong W, Kenny JM, Ma P (2019) Poly(lactic acid)/lignin films with enhanced toughness and anti-oxidation performance for active food packaging. *Int J Biol Macromol*. <https://doi.org/10.1016/j.ijbiomac.2019.12.08>
35. Long-Feng W, Jong-Whan R (2016) Grapefruit seed extract incorporated antimicrobial LDPE and PLA films: Effect of type of polymer matrix. *LWT* 74:338–334
36. Roy S, Rhim JW (2020) Preparation of carbohydrate-based functional composite films incorporated with curcumin. *Food Hydrocoll* 98:105302

**Publisher's Note** Springer Nature remains neutral with regard to jurisdictional claims in published maps and institutional affiliations.

Springer Nature or its licensor (e.g. a society or other partner) holds exclusive rights to this article under a publishing agreement with the author(s) or other rightsholder(s); author self-archiving of the accepted manuscript version of this article is solely governed by the terms of such publishing agreement and applicable law.

## Authors and Affiliations

Usman Lawal<sup>1,2,3</sup> · Vijay Robert<sup>1</sup> · Akshai Gopi<sup>1,2</sup> · Sravanthi Loganathan<sup>1,2</sup> · Ravi Babu Valapa<sup>1,2</sup>

✉ Ravi Babu Valapa  
vravibabu@ceciri.res.in; vravibabucecri@gmail.com

<sup>1</sup> Electrochemical Process Engineering Division, CSIR-Central Electrochemical Research Institute (CECRI), Karaikudi, Tamil Nadu 630003, India

<sup>2</sup> Academy of Scientific and Innovative Research (AcSIR), Ghaziabad 201002, India

<sup>3</sup> Department of Chemical Sciences, Federal University Wukari, Taraba, Nigeria